Journal of Computer-Aided Molecular Design, 11 (1997) 491–501.
KLUWER/ESCOM
© 1997 *Kluwer Academic Publishers. Printed in The Netherlands.*

J-CAMD 412

Comparative molecular modelling study of the calcium channel blockers nifedipine and black mamba toxin FS_2

Klaus-Jürgen Schleifer

Institute for Pharmaceutical Chemistry, Heinrich-Heine-Universität Düsseldorf, Universitätsstrasse 1, D-40225 Düsseldorf, Germany

Received 28 January 1997
Accepted 16 May 1997

Keywords: Snake toxins; Angusticeps toxins; Nifedipine; Calcium antagonist; 1,4-Dihydropyridine; Voltage-gated calcium channel

Summary

The identification and structural determination of the critical amino acid residues causing the calcium channel blocking effects of the angusticeps type III toxin FS_2 is described. Alignments with more than 200 different short and long neuro-, cyto-, muscarinic and other angusticeps-type toxins yielded 12 amino acid residues at the tips of loops II and III which are unique to the type III toxins. The competitive binding behaviour between the 1,4-dihydropyridine derivative nifedipine and toxin FS_2 was used for a further delimitation of the relevant toxin binding domain. Using the ab initio geometry optimized nifedipine X-ray structure as a template, a model based on the sequence Met^{45}-Trp^{46}-*cis*-Pro^{47}-Tyr^{48} has been elaborated. This sequence shows the same hydrophobic and hydrogen bond forming properties as nifedipine. In addition, qualitatively similar molecular electrostatic potentials are observed for both structures, leading to the assumption that these amino acid residues of the toxin act as the potential attachment region at the calcium channel receptor site.

Introduction

Snake venoms comprise an almost inexhaustible pool of physiologically active compounds. The Elapid snake venoms (cobras, mambas and ringhals families) show a multitude of diversely acting toxins [1]. These small peptides, consisting of 58–74 amino acid residues, can easily be aligned using four pairs of cysteines (five pairs in long neurotoxins) which form the following intramolecular disulphide bridges: 1st Cys–3rd Cys, 2nd Cys–4th Cys, 5th Cys–6th Cys and 7th Cys–8th Cys (Fig. 1). Together with an extensive β-sheet arrangement within the antiparallel loop regions, the same three-finger architecture occurs in all of these toxins, even though their effects may be quite diverse.

The spectrum of pharmacological effects ranges from inhibition of the postsynaptic nicotinic acetylcholine receptor (short and long neurotoxins), and changes of membrane permeability (cyto- or cardiotoxins), to agonistic and antagonistic effects on the muscarinic acetylcholine receptor (two different types of muscarinic toxins). Besides these highly poisonous families, a fourth class, named *angusticeps*-type toxins, has been first isolated from the green mamba Dendroaspis angusticeps [2]. They show no neurotoxic or cytotoxic capability and only a very weak lethal character when tested alone, but a synergistic enhancement is generally observed when they are used in combination with other components of the same venom [2]. Well-defined activities have been determined for only two of the four subgroups. In particular, the fasciculins (representing subgroup I) act as specific inhibitors of the acetylcholinesterase, whereas the black mamba toxins calciseptine and FS_2 (which belong to subgroup III together with the toxins C10S2C2 and S4C8) have been demonstrated to block L-type calcium channels [3,4]. In vitro investigations with calciseptine and toxin FS_2 showed a dose-dependent relaxation in pre-constricted rat aorta, pulmonary artery and trachea with a similar onset and duration pattern as that of the 1,4-dihydropyridine derivative nifedipine. In addition, calciseptine was shown to relax the contraction of rat aorta provoked by the L-type channel agonist Bay k 8644. This relaxation was not affected by propranolol, indometacin and N^G-nitro-L-arginine [5]. In vivo studies on anaesthetized rats found

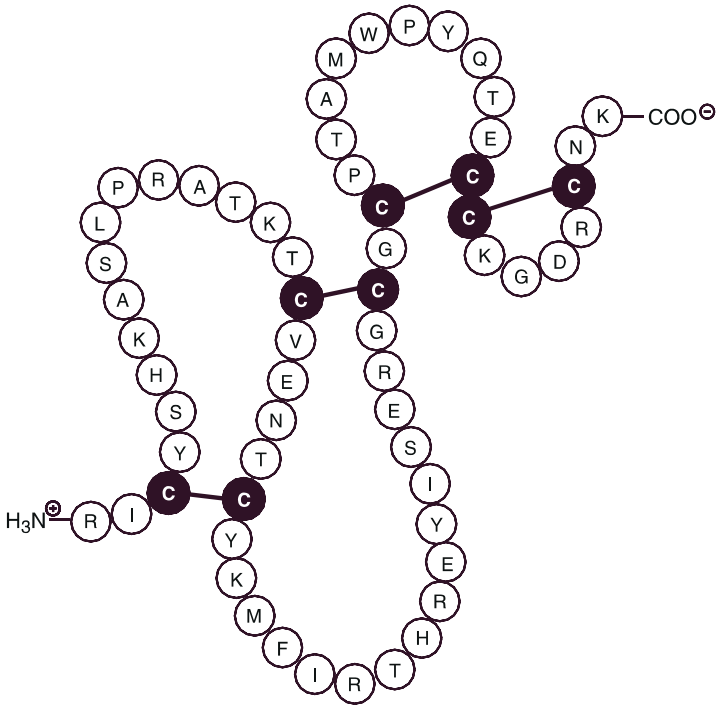

Fig. 1. Sequence of toxin FS_2 with the typical cysteine bonding pattern of three-finger toxins (the one-letter code for amino acid residues is used).

calciseptine and FS_2 to have more potent and sustained depressor effects than nifedipine [5]. Biochemical investigations with the radiolabelled nifedipine analogue [^{3}H]nitrendipine showed a competitive binding with FS_2 at the α_1-subunit of the L-type voltage-gated calcium channel (VGCC). Moreover, allosteric behaviour at the benzothiazepine ([^{3}H]diltiazem) and phenylalkylamine ([^{3}H]verapamil) binding sites similar to that of 1,4-dihydropyridines was observed [6].

What follows is a theoretical approach to deduce the specific amino acid residues responsible for the calcium channel blocking effects of angusticeps type III (AT-III) toxins. Applying different molecular modelling strategies, the essential molecular properties of these residues will be characterized using nifedipine as a template. A comparison of the physicochemical features of the hydrophilic toxin FS_2 (18 charged amino acids) with the hydrophobic nifedipine molecule provides unique insight into the bind-

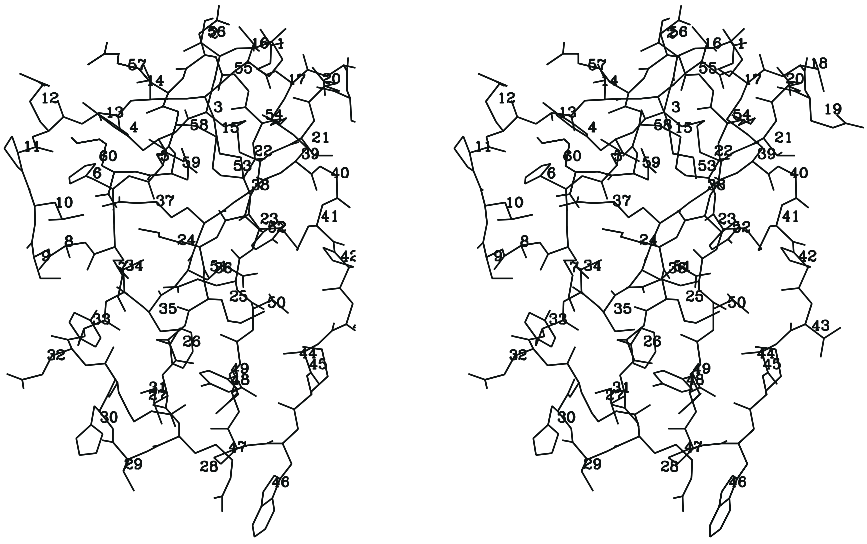

Fig. 2. Stereoplot of the 3D solution structure of toxin FS_2. Only heavy atoms of conformation 14 (Brookhaven code 1tfs [12]) and the corresponding sequence numbers are shown.

ing characteristics of both the AT-III toxins and the therapeutically used 1,4-dihydropyridines with the L-type VGCC.

Materials and Methods

Hardware and software

All computations were carried out on Silicon Graphics Indigo^2 workstations using the molecular modelling software package INSIGHT II/DISCOVER [7]. In order to detect potential interaction fields of toxin FS_2 or nifedipine being essential for the binding at the receptor site the program GRID [8] was used. GRID computes the interaction energies of a specific probe molecule with well-defined properties at different grid points over the van der Waals surface of the target molecule. The visible grid fields indicate energetic favourable, accessible regions of the examined molecule. To compare common GRID regions of toxin FS_2 and nifedipine with the same probe molecule, the program GRAD [9] was applied. DelPhi calculations [10] were carried out to compute and visualize the molecular electrostatic potential (MEP) of the molecules. All hardware and software were provided by Prof. H.-D. Höltje at the Freie Universität Berlin and the Heinrich-Heine-Universität Düsseldorf, respectively.

Alignment strategy

The original sequence of toxin FS_2 [11] was corrected at position 32 according to the experimental NMR results of Albrand et al. [12], which show resonances for glutamate (E) instead of the expected ones for glutamine (Q) at this position (Fig. 1). Multiple sequence alignment was used to determine the conserved amino acid residues within each toxin family and to identify those residues which are exclusive to the AT-III family. Taking one sequence of an AT-I, AT-III, neuro-, cyto- and muscarinic toxin at a time, the program MaxHom [13] was applied using the automatic server for *P*rofile fed neuronal network systems from *H*ei*D*elberg (PHD) [14] at the European Molecular Biology Laboratory. MaxHom searches similar sequences in the SWISSPROT database [15] and aligns them automatically. For example, in the case of the long neurotoxin α-bungarotoxin, 150 sequences with identities ranging from 69% to 34% were aligned. The expression 'unique amino acids' will be used if identical amino acid residues within one family are found no more often than in 5% of all other aligned toxins.

Toxin FS_2

The coordinates of 20 conformers of toxin FS_2 elucidated by NMR spectroscopy (pH 5.3 in 99.6% D_2O or 90% H_2O/10% D_2O; PDB entry code 1tfs [12]) were extracted from the Brookhaven Protein Database [16] (Fig. 2). To investigate the toxins under physiological conditions, pH 7.4 was chosen for all computations. Each conformer was adjusted to the consistent valence force field (CVFF) [7] by using 25 iterations of the steepest descent minimization procedure. During the first 20 steps the backbone atoms were fixed; afterwards, an unrestricted mobility of all atoms was allowed. To guarantee the intactness of the experimental NMR structure, the relax-

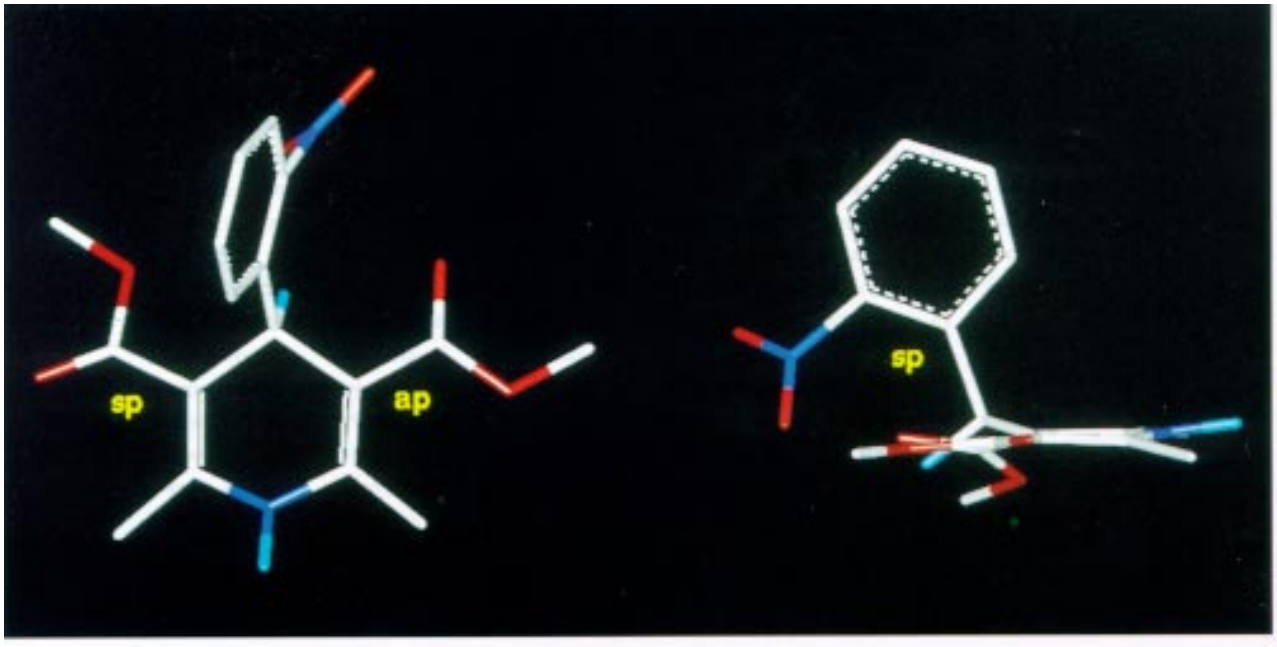

Fig. 3. X-ray structure of nifedipine [20], coloured by atom type: carbons white, oxygens red, nitrogens blue and hydrogens cyan. For clarity, only the hydrogens in positions 1 and 4 are shown (sp, synperiplanar; ap, antiperiplanar).

a

```
ALIGNMENTS    1 - 99
 SeqNo    ....:....1....:....2....:....3....:....4....:....5....:....6....:....7....:....8....:....9....:...10
     1    RRRRR RRR R   RR         RRRR     RRRR K  R                         R                           R R
     2    IIIIIIIII IIIIRR   I   IIRIRR     RRRI I  I      II         I    I  I                 M         I E
     3    CCCCCCCCCCCCCCCC CCCCCCCCCCCCCCCCCCCCCCC  CCCCCCCCC         CCCCCCC C                CC         C C
     4    YYYYYHYYYHYYYHYF HHYHHHHHYFFFHHCCHFFFYHY  YHHCCCCYY         FCCCCYC Y                VY         L Y
     5    SISTNNNNNNSSSNNN NNSNNNNNNNNNNNNNNNNNNNN  INNNNNNKKEE       NNNNNSN N                TS         NEL
     6    HHHHHQHHHQHHHQQHHQQHQQQQQQHHHQQQQQQQQHQQ  AQQQQQQQQCC       QQQQQHQHH          HHHH  GH      HHHQCN
     7    KKKKQQQQQQKKKQQPNQQKQQQQQQQPPQQQQMQQQLQPKN.QQQQQQQRNNNNNNNNNEQQQQTQNLNNNNNKNNHHNNNN  KTHNNHHNNNNQN.
     8    AAASSSSSSSLTTSSSRSSTSSSSSSSSSSSSSSSSSGSSKK.SSSSSSsKQKKKKKKKTSSSSTSKGQKKKKKKQKKKKTT  STQQQQKKTTTQK.
     9    SSSLNSTTTSLPPSSSPSSPSSSSSSSSSSSSSSASSSTSSLL.ISSSSSqqLLLLLLLLLYSSSSTSVTLLLLLLLLLLLLQQ  ITLLLLLLPQQSL.
    10    LLLQTQTTTQQQQQQQLQEQQQQQQQQQQQQQQQQQQQKQQIV.QQQQQQFFVIIIIIIIIRQQQQSQVKIVVVVVVIVVVVLLVIGSVIIIVVLLLTV.
    11    PPPAPPRPPPANPPPPPPPNPPPRPPPPPATPPPPPPPTHPPPTPPPPPPPPPPPPPPPPPPPPPRPPPPPPPPPPPPPPPPPPPGRPPPPPPPPPPPP
    12    RRRKAPAAAPKSSPKQFPPSPPPPPKQQQPPKKPKQQPPPLIYPPKKKKIIIIILLLILLEKKKKAKFPPLLLLLLPPPFFFFPPIAPPPPPLFFFeIH
    13    AAATTTTTTTTAATTTLTTATTTTTTTTTTTTTTTTTTTTTFADTTTTTTTTAAAAAAAAATTTTTITLTFFFFFFFFVVLLIIFFSIFFFFFFIIInAD
    14    TTTTTITTTTTTTITNHTTTTTTIITTNNTTTTTTNNTTTSYHTTTTTTTTHHYYYYSYYTTTTTLTSTYYYYYSYYWWSSYYWWTLWWWWWYYYYGHT
    15    KKKKKKKKKKKIIKKKKKTIKKKKKKKKKKQTTTKKKETKKKKTTTTTTVVKKKKKKKKKTTTTTKTKEKKKKKKKKKKKKKKKKETKKKKKKKKNQKQ
    16    TTTSSTSSSTTTTTSSTTRTSTTTTSTSSTTTDRSSSTGATTTGHNDIDCCTTTTTTTTTTNNNDDNTCTTTTTTTTTTTTTTTTENTTTTTTTTTCTT
    17    CCCCCCCCCCCCCCCCCCCCCCCCCCCCCCCCCCCCCCCCCCCCCCCCCCPPCCCCCCCCCCCCCCCCCTCCCCCCCCCCCCCCCCCCCCCCCCCCCYCC
    18    VVVEVSEGGpEEEpppPssEPpppppsppspPAspppQspPPassAAaAGGPPPPPPPPPPAAAAGAPQAPPPPPPAPPPPPPPPaGPPPPPPPPPIPp
    19    EEEGEEEEEeEEEeeeeeeEGeeeeeeeeeegDeeeeEeeeeeeeGDeDEEeeeaaaaaaDEEEDEEeEaaaaaaaaeeedeeeeqEekkeeaeeeKaq
    20    NNNNNGNNNTNKKTNNnTTKDTTTTNSNNTTsNTNNNDTKnnNTTNNSNKKnnnnnnnnngSSSDNSnDnnnnnnnnnnnnnnnnKNnnnnnnnnnTnE
    21    TTSTSQSSSNSTTNSSINNTtNNNNSSSSNNSSNSSSSNNLLINNSSSSNNLLLLLLLLLnSSSSSSLSLLLLLLLLLLLLLLLLISLLLLLLLLLDLI
    22    CCCCCCCCCCCCCCCCCCCcCCCCCCCCCCCCCCCCCCCCCCCCCCCCCCCCCCCCCCCCCCCCCCCCCCCCCCCCCCCCCCCCCCCCCCCCCCCCCCC
    23    YYYYYYYYYYYYYYYYYYYYYYYYYYYYYYYYYYYYYYYYYYYYYYYYYYYYYYYYYYYYYYYYYYYYYYYYYYYYYYYYFFYYFYYYYYYYYFFFQYY
    24    KKKKKKKKKKKKKKNNKKKKNKKKKNNNNKKKKKNRRKKRKKLKEKKKKKKKKKKKKKKKKSKKKKRKKKKKKKKKKKKKKKKKKKKRKKKKKKKKKNQV
    25    MMMMSKKKKKRKKKKKMKKFKKKKKKKKKKKKMKKKKNKKMMKKKKKKKKKMMMMMMMMMTKKKKKKMNMMMMMMMMMMMMMTAMMKKMMMMMMGAAKMK
    26    FFFFITYTTVSFSQQQTWRVRQRRRQQQQWQTTRQQQIRQTFARRTTTTQQFFMFFYFFFFTTTTSTTIFFFFFFFFFFFTSTTYTWSYTTYYYTTTTYS
    27    IIIIWWWWWWLVVWWWLWWTWWWWWWWWWWWWWWWWWWWWWWMMWWWWWWWWWWMMLMMMMMMWWWWWRWLWMMMMMMMMMMMMLLMMTRMMMMMMLLLWMW
    28    RRRRARRSSRPTRRRRKSRKRSRRRRSRRSSRRRRRRTRSRMcRHSQSKSSVVAVVVMVVHSSRKRSKRVVVVVVVVVVLEKKVRKRVRRVVVKKKNVc
    29    TTTTDDDDDDKNKDDDKDDLDDDDDDDDDDDDDDDDDDDFDDLSsDDDDDDGGSSSASSSSSNDDDDHDKNASSASAAASSKVKKSLmHSGAAAAFKFTSs
    30    HQSSHHHHHHIVLHHHTHHPHHHHHHFHHHHHHHHHHHDHHADSHHHHHHHHTTKANNDNNDHHFHPHVIANNTNATATTMTLFTApPSAATTTPFPHKS
    31    RRPRRRRRRRPPPRRRPRRGRRRRRRRRRRRRRRRRRRNRRPLRRRRRRRRRSSKPKKLKKGRRRRPRPTPLKPLPPPSSPPPPLPKPSSPPPPKPLRSR
    32    EEDEGGGGGGGLGAGGGMGG.GGGGGGGGGGGGGGGGG.GGKTGGGGGGGGGGTTMKTTTTTHGGGGKGKFKTMKTHKKTTKMLLTKLKTKMMMKKlKGTG
    33    YYYYTTTTTTIVITSTKTYVTTSTTSTTTTSTTYSTT.YTVIKYTTTSTTTVVVVVVIVVVTTTTMTIDVVVVVVVVVVIIKKVVYMVVVILVIfFSIK
    34    IIIIIIIIIIIIVIIILIRIIIIIIIIIIIIRIRKIIIIRIPPKRIIRRRIIPPPPPPPPPKRRRRVRPNPPPPPPPPPPPPiiPPDVPPPPPPTPPRPV
    35    SSSSISIIIIILAITIsITLIITIITITIITIITTIIITIVVLTIIIITIIIVVVVVVVVVIIIIILIIIVVVVVVVVVVIIiiVVVLVVVVVVYVVTVL
    36    EEDEKEEEEEGAGEEEkEEAEEEEEEEEEEEEEEEEEEREEKKEEEEEEEEEEKKKKKKKKKEEEEEGEKRKKKKKKKKKKKKKKKSGKKKKKKKKKDKE
    37    RRRRRRRRRRRRRRRRRRRRRRRRRRRRRRRRRRRRRRRRRFRRRRRRRRRRRRRRRRRRRRRRRRRRRRRRRRRRRRRRRRRRRRRRRRRRRRRRRRF
    38    GGGGGGGGGGGGGGGGGGGGGGGGGGGGGGGGGGGGGGGGGGGGGGGGGGGGGGGGGGGGGGGGGGGGGGGGGGGGGGGGGGGGGGGGGGGGGGGGGGG
    39    CCCCCCCCCCCCCCCCCCCCCCCCCCCCCCCCCCCCCCCccCCCCCCCCCccccccccccCCCCCCCcCcccccccccccccCccccCccccccccCCcC
    40    GGGGGGGGGGGGGGGGGaGGGGGGGGGGGGGGGGGGGGGGGGvvaGGGGGGGGvvvavvvavGGGGGGGaGvvvvvvvvvvvatanvvtGvvvvvvanaGva
    41    CCCCCCCCCCCCCCCCcCCCCCCCCCCCCCCCCCCCCCCCCcCCCCCCCCCCCCCCCCCCCCCCCCCCCCCCCCCCCCCCCcCCCCCCCCCCCCCcCCc
    42    PPPPPPPPPPPPPPPPPPPPPPPPPPPPPPPPPPPPPPPPPFPPPPPPPPPPPPPPPPPPPPPPPPPPPPPPPPPPPPPFPPPPPPPPPPPPPPPPPPPPP
    43    TTTTRTKKKTLKSSTTSKTkTSSSSKTQQKTRQTKTTTSTKKTSTQQHQSSKKKKKKKKKRQQQQPQKTKKKKKKKKKKKKKKKKKKPKKKKKKKKKRKKS
    44    AAAAVVVVVVTKKVVVEVVeVVVVVVVVVVVVVVVVVVVPVVSNVVVVVVVVVVDNNNNNNNNNVVVVVGVSPSNSSNSSSDNSSSNNSAGNSSNDSTNSVSV
    45    MMMM.KKKKKLEEKKKRKKIKKKKKKKKKKKKKKKKKKRKKSSKKKKKKKKKKSSSSSSSSSSNKKKKDKSRSSSSSSSSSSSSSSSSSDDSSSSSSSSSSKSN
    46    WWWW.PPRQPPIMKPPPPKFPKKKKPPSSPPPPKPPPGNPFLPNPSPPPKKAAALLLLLLPSPPPDKLGLALLALLLAALLAAALEDALLAALAASPLT
    47    PPPPKGGGGGFFLGGGLGGRGGGGGGGGGGGGGGGGGDGGLLGGGGGGGGGLLLLVVLLLPGGGGYGLDLLLLLLLLLLLLLLLLYYLLLLLVLLLGLG
    48    YYYYSIVVIILRVVIIVVIKIVIVVIIIIVIIIIIIVMIVVVVIVIIIIIIVVVVLLVVVIIIIILIVMVVVVVVVVVVVVVLLVIGLVIIVVLVLVIVT
    49    QQQQKHGHHKRSAGKKQNESNKEGGKKKKKKRKQKKKPEKKKDEKKKKKEEKKKKKKKKK.KKKKEKNPKKKKKKKKKKKKKKKKCEKKKKKKKKKNKE
    50    TTTTIIILLLIIIILLVLLILIIIILLLLLLLLLLgILYYIILLLLLIIYYYYYYYYYSLLLLVLVgYYYYYYYYYYVVVVYYYVVYYYYYYYYYVLYI
    51    EEAEKSHHHNKHHYRRENNHKNNYYRSTRNKIEHRRRyNHEVSNNEETENNVVVVVEVVVIEEEEKEMyVVVVVVVVVVVVVVVMKKVMMMMVVVVRVK
    52    CCCCCCCCCCCCCCCCCCCCCCCCCCCCCCCCCCCCCCCCCCCCCCCCCCCCCCCCCCCCCCCCCCCCCCCCCCCCCCCCCCCCCCCCCCCCCCCCCCC
    53    CCCCCCCCCCCCCCCCCCCCCCCCCCCCCCCCCCCCCCCCCCCCCCCCCCCCCCCCCCCCCCCCCCCCCCCCCCCCCCCCCCCCCCCCCCCCCCCCCCC
    54    KKKKKAQQQTTRRKEQKRTRTTTKKEEQQRTKKTEQQETTDNDTTHKKKTTNNSNNNNNNKHHHKtHKENNNNNNNNNSSNKSSNNKtNNNNNNNSKKNS
    55    GGGGSSSSSTSSSTSSTTTSTTTTTSSSSTTTTSSSSSTTTTTTTTTTTTTTTTTTTTTTTTTTTTpTTSTTTTTTTTTTKTTTTTTpTTTTTTTTTTTA
    56    DDDDDDDDDDDDDDEDDDDDDDDDNEEDDDDDNDEEEDDEDDDDDNNDNDDDDDDDDDDDDNNNNDNDDDDDDDDDDDDDDDDDNDDDDDDDDDDDDDD
    57    RRRRNKKKKKKKKKDDKRRKRRKKKDVDDRREENDDDKRKKRNRKEEEEKKRRRRRRRRRKEEEEKEKKRRRRRKRRKKKKKKKKRKKKKKKRKKKKRK
    58    CCCCCCCCCCCCCCCCCCCCCCCCCCCCCCCCCCCCCCCCCCCCCCCCCCCCCCCCCCCCCCCCCCCCCCCCCCCCCCCCCCCCCCCCCCCCCCCCCCC
    59    NNNNNNNNNNNNNNNNNNNNNNNNNNNNNNNNNNNNNNNNNNNNNNNNNNNNNNNNNNNNNNNNNNNNNNNNNNNNNNNNNNNNNNNNNNNNNNNNNNN
    60    KKKK   NNN EERNN NNENNNRRNNNNNKNNNNNNN NN   NNNNNNRR         NNNNN N                K          E
```

b

1 : txf2_denpo	18 :nxs1_najox	35 :nxsd_latco	52 :cx9_najha	69 :tx51_denja	86 :tsyl_denan
2 : txca_denpo	19 :nxs1_najmo	36 :nxsc_latcr	53 :cx10_najha	70 :cxn_najat	87 :txf7_denan
3 : tx02_denan	20 :tx49_denvi	37 :nxsc_latla	54 :cx4_najmo	71 :cx4_najat	88 :cx5_najhh
4 : tx48_denja	21 :nxs1_hemha	38 :mamb_denja	55 :cx5_najka	72 :cx5_najat	89 :cx2_najmo
5 : tx50_denja	22 :nxs1_najme	39 :nxs1_najat	56 :cx3_najna	73 :cx1_najsp	90 :cx1_najpa
6 : nxs1_micni	23 :nxs1_najha	40 :nxs1_bouan	57 :cx1_najna	74 :cx2_najat	91 :cx2_najni
7 : nxs1_denpo	24 :nxs2_najni	41 :cx5_najmo	58 :cx1_najat	75 :cx2_najox	92 :cx2_najha
8 : nxs1_denvi	25 :nxs2_najha	42 :cx1_najox	59 :cx3_najka	76 :cx3_najat	93 :cx2_najna
9 : nxs1_denja	26 :nxsc_latco	43 :nxl1_aspsc	60 :cx2_najka	77 :cx6_najat	94 :cx3_najme
10 :nxs1_najpa	27 :nxs1_latse	44 :nxs1_najka	61 :txw1_ophha	78 :cx1_najni	95 :cxh_najna
11 : tx31_denan	28 :nxsb_latla	45 :nxs1_bouch	62 :nxs2_enhsc	79 :cx1_najha	96 :cx7_najat
12 :tx54_denja	29 :nxsb_latcr	46 :nxs1_astst	63 :nxs1_enhsc	80 :cx1_hemha	97 :nxs1_bunfa
13 :txf8_denan	30 :nxs1_najph	47 :nxs1_aipla	64 :nxs1_hydla	81 :cx3_hemha	98 :cx1_najme
14 :nxs2_najhh	31 :nxs2_hemha	48 :nxs1_pseau	65 :nxs4_aipla	82 :cx11_najha	99 :nxl1_latse
15 :nxs2_latco	32 :nxs1_acaan	49 :nxs3_aipla	66 :txac_denpo	83 :cxh_najka	
16 :nxsa_latcr	33 :nxs2_aipla	50 :nxs3_najha	67 :nxs1_hydcy	84 :cx3_najha	
17 :cxh_hemha	34 :nxs3_najmo	51 :nxs4_najha	68 :cx2_hemha	85 :cx3_najmo	

Fig. 4. (a) Sequences and MaxHom alignment [13] of three-finger toxins showing the AT-III toxins in columns 1–4 (pairs of lower-case characters (AvaK) bracket a point of insertion and dots (...) represent points of deletion in this sequence). (b) SWISSPROT entry codes for #1–99.

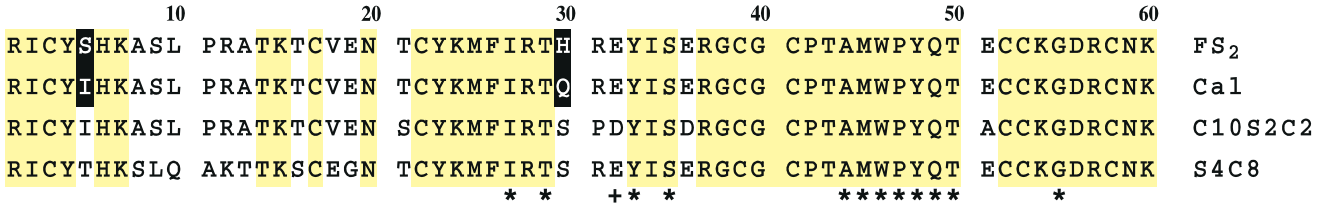

Fig. 5. Alignment of AT-III toxins FS_2, calciseptine (Cal), C10S2C2 and S4C8 (identical amino acid residues are underlaid; ∗, unique residues which are exclusively found in this family; +, conserved 'functional unique residue'; white letters, sequence differences among toxin FS_2 and calciseptine).

ation was stopped before the heavy atoms showed rms deviations larger than 0.05 $Å^2$. In addition, the intramolecular hydrogen bonds were calculated before and after the geometry optimization. The stereochemical accuracy of all peptide parameters was checked with the program PROCHECK [17] and the Connolly algorithm was used to determine the solvent accessible surface [18]. The partial charges out of an ab initio single point calculation using the 6-31G* basis set and the ESP method within the SPARTAN software package [19] were used for the MEP computation of the toxin FS_2 fragment (see Fig. 14). In contrast to the topological CVFF atomic charges, the quantum chemical method considers the special conformational status of this peptide.

Nifedipine

The X-ray structure of nifedipine (reference code BICCIZ [20]) was copied from the Cambridge Structural Database [21]. Considering further 34 X-ray structures of 1,4-dihydropyridine (DHP) derivatives emphasized that the DHP ring exists in crystals in an unusual boat form (Fig. 3). The ester groups show an almost coplanar orientation. The 4-aryl substituent points in a pseudoaxial direction approximately bisecting the heterocycle. In relation to the double bonds of the DHP ring, the carbonyl groups of the ester side chains can be oriented in a synperiplanar (*Z*)-conformation (sp) or an antiperiplanar (*E*)-conformation (ap). Also, for the relative spatial orientation of the 2'-nitro group and the hydrogen in position C4, the terms sp and ap are used if both are pointing to the same or opposite direction, respectively. Following earlier experimental [22] and theoretical results [23,24] indicating the C3-sp, C4-sp and C5-ap orientations as the putative pharmacophore conformation of DHPs, the nifedipine X-ray structure was chosen for further investigations. To eliminate short atom–atom contacts and conformational distortions produced by intermolecular interactions in the crystal lattice, an ab initio geometry optimization was carried out using the 3-21G* basis set [19]. To avoid the use of inaccurately parametrized, topological partial charges of the force field (CVFF), the wave function of the minimized output structure was recomputed with the 6-31G* basis set [19] to derive the atomic charges.

Results

Multiple sequence alignment

The alignment initiated with the sequence of toxin FS_2 revealed 99 peptides with amino acid identities ranging from 95% to 35% (Fig. 4). It comprises the four AT-III toxins, short and long neurotoxins and cytotoxins. To also take into account the fasciculins and muscarinic toxins, this procedure was repeated using as input the sequences of fasciculin 1 and the muscarinic toxin MT 1 (not shown).

A close inspection of the results indicates 44 amino acid residues (74%) within the AT-III family to be identical but only 12 of them as being unique (Fig. 5). In contrast to 18 ionic residues of toxin FS_2 leading to a net charge of +6, these unique residues are not charged and

TABLE 1
CHARACTERISTICS OF THE INVESTIGATED SOLUTION CONFORMERS (#1–20) OF TOXIN FS_2

FS_2 conformer #	Hydrogen bonds		
	Experimental	Minimized	Extra
1	56	55	7
2	49	50	7
3	60	60	5
4	57	57	5
5	54	53	6
6	63	62	7
7	49	48	5
8	62	63	8
9	62	64	8
10	52	52	9
11	55	56	8
12	61	60	8
13	55	55	8
14	58	56	9
15	57	57	6
16	58	61	8
17	59	59	7
18	59	61	7
19	65	63	7
20	57	58	9

The number of hydrogen bonds are indicated: (i) experimental, NMR structure; (ii) minimized, force field geometry optimized structure; and (iii) extra, out of the maximum of 10 supplemental hydrogen bonds the number of detected bonds in the corresponding conformer.

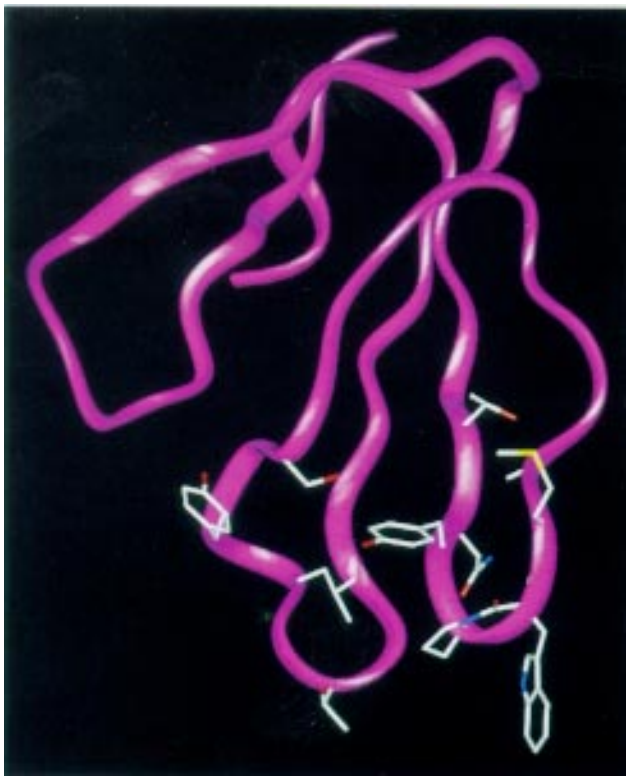

Fig. 6. Trace of toxin FS_2 showing unique amino acid residues of AT-III toxins (hydrogens are not displayed) (coloured by atom type: carbons white, oxygens red, nitrogens blue and sulphur yellow).

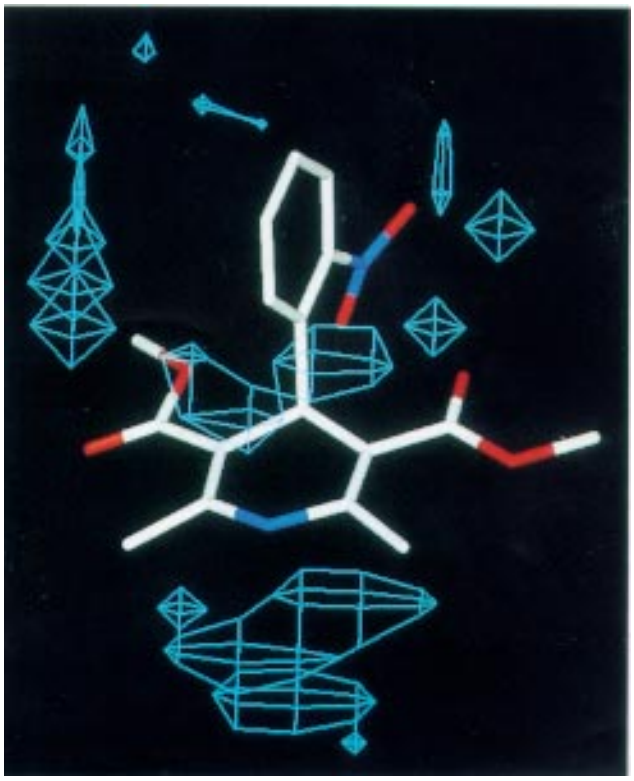

Fig. 7. Hydrophobic interaction fields from nifedipine using the hydrophobic probe molecule of GRID [8] contoured at –0.5 kcal/mol.

Fig. 8. Ribbon representation of toxin FS_2. Grids show energetically favourable interaction fields generated with the hydrophobic probe of GRID [8] (contoured at –1.4 kcal/mol). A yellow dashed line indicates the type VIa *cis*-proline turn-stabilizing hydrogen bond formed by the Met^{45} carbonyl oxygen and the Tyr^{48} amide hydrogen which fixes the Trp^{46}-*cis*-Pro^{47} topology.

five of them show hydrophobic character (Ile^{27}, Ala^{44}, Met^{45}, Trp^{46} and Pro^{47}). Additionally, all AT-III toxins possess an aspartate (D) or glutamate (E) in position 32, which is not found in any other sequence.

Determination of the toxin FS_2 3D reference conformation

In order to transfer the results onto a 3D structure, one representative conformation out of 20 minimized

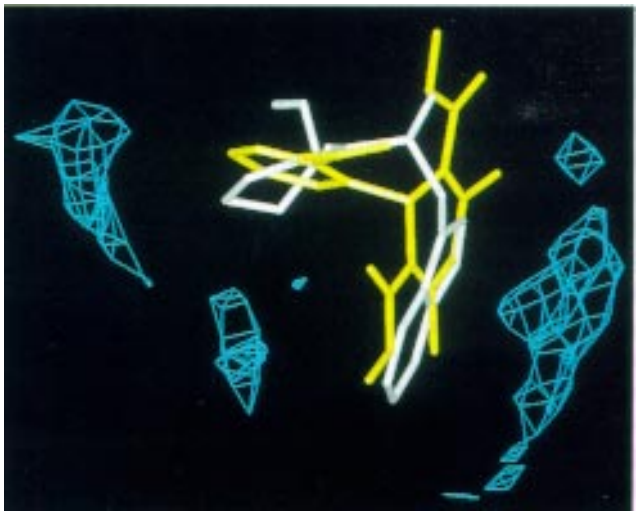

Fig. 9. Superposition of nifedipine (yellow) and the Trp^{46}-*cis*-Pro^{47} sequence of toxin FS_2 (white). GRAD [9] fields indicate common energetically favourable hydrophobic regions of both structures.

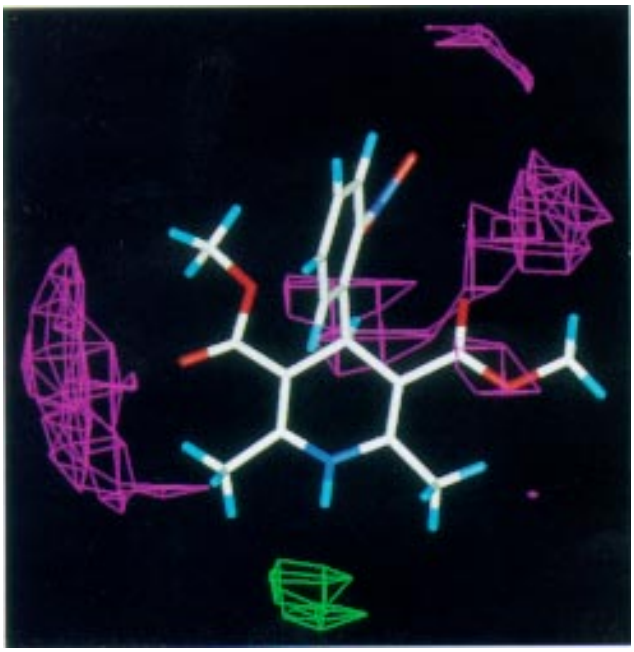

Fig. 10. Hydrogen bond acceptor (magenta) and donor sites (green) of nifedipine contoured at –3.0 kcal/mol.

NMR conformers of toxin FS_2 should be chosen as reference. Since the conserved topology of three-finger toxins is generated by an extensive β-sheet secondary structure, stabilized by intramolecular hydrogen bonds between antiparallel oriented backbone atoms, the number of hydrogen bonds was determined for each conformer (see Table 1).

A quantitative evaluation of all hydrogen bonds shows differences between the individual conformers. For example, conformer 9 contains 64 hydrogen bonds whereas conformer 7 shows only 48 hydrogen bonds. The qualitative analysis indicates, for each conformer, 20 highly

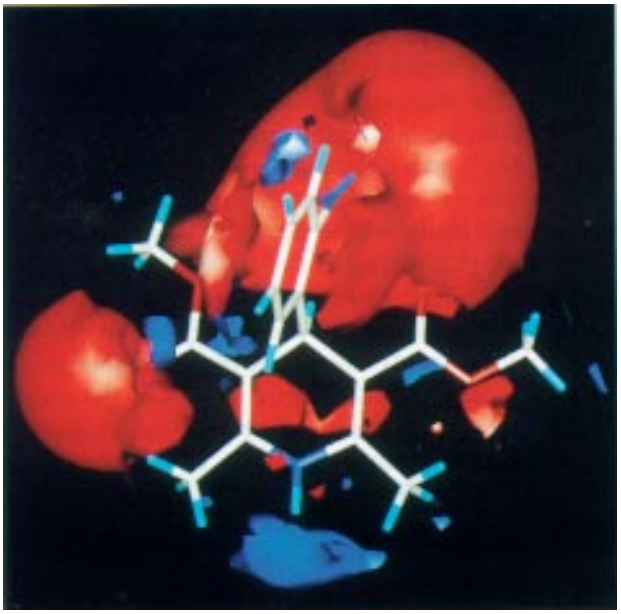

Fig. 12. MEP of nifedipine (red clouds represent a negative potential of –0.5 kT/e and blue clouds represent a positive potential contoured at 1.0 kT/e).

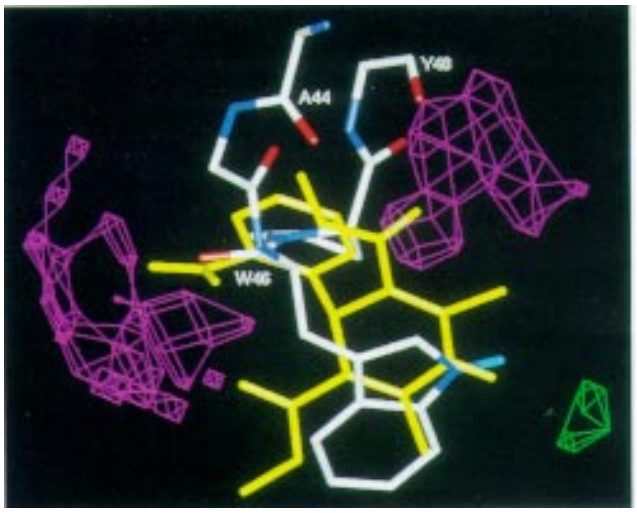

Fig. 11. GRAD [9] fields indicating common hydrogen bond acceptor (magenta) and donor regions (green) of the fitted toxin FS_2 (coloured by atom type) and nifedipine (yellow). The acceptor carbonyl oxygens of the toxin are labelled (A44, alanine; W46, tryptophan; Y48, tyrosine). Only the donor hydrogens of the indole and DHP rings are shown.

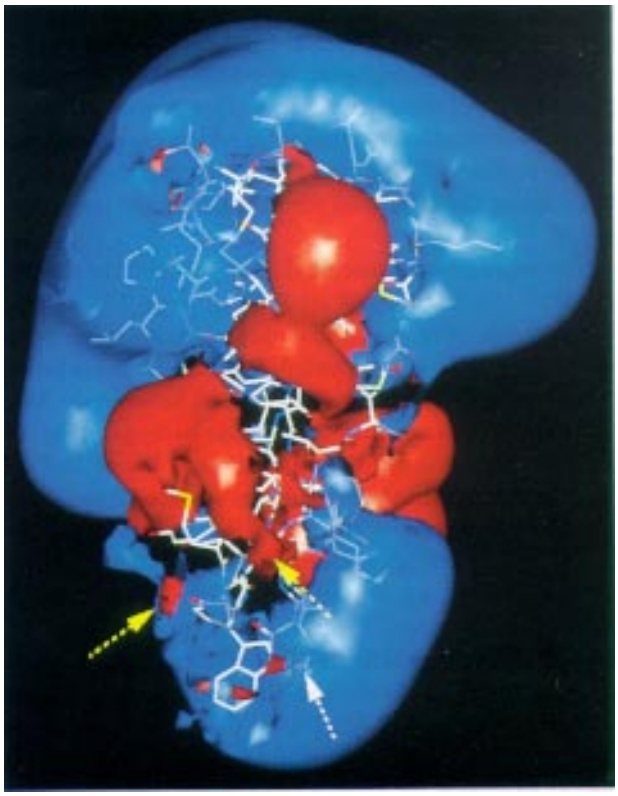

Fig. 13. MEP of toxin FS_2 (red clouds represent a negative potential of –0.5 kT/e and blue clouds represent a positive potential contoured at 1.0 kT/e). Yellow arrows indicate the negative potentials induced by the Trp^{46} (left) and Ala^{44}/Tyr^{48} (right) backbone carbonyl oxygens. The white arrow shows the charged Arg^{28} guanidinium side chain.

conserved hydrogen bonds that stabilize the three-finger secondary structure. In addition, 10 extra hydrogen bonds are detected in at least 10 conformers (means ≥50%). The reference conformer should contain as many as possible of these supplementary hydrogen bonds. Since conformers 10, 14 and 20 show the same high score of nine additional hydrogen bonds, the lowest potential energy conformer 14 was selected as the reference conformation. To check its conformational parameters, all peptide geometries were investigated with PROCHECK [17]. The Ramachandran plot [25] of conformer 14 (not illustrated) shows the phi (C^{α}-C) and psi (C^{α}-N) angles of 41 residues (78.8%) to be optimal, nine residues (17.3%) to be allowed, and only Ala^{8} and Arg^{57} (3.8%) to be in the generously allowed region, whereas no residue is found in disallowed regions.

Molecular properties of nifedipine and toxin FS_2

When the alignment results are transferred onto the 3D reference structure, all unique residues of AT-III toxins are found at the tips of loops II and III, exposed to the solvent accessible surface of the molecule (Fig. 6).

To further delimit the essential residues causing the calcium channel blocking effects, the characteristic properties of nifedipine will be used as templates. One of the most striking features of this 1,4-dihydropyridine derivative is its strong lipophilicity. Nifedipine is almost insoluble in water (6 mg/l), and shows a distribution coefficient in octanol/water of 10000:1 [26]. To quantify and visualize these hydrophobic properties, the hydrophobic probe DRY of program GRID [8] was used. Figure 7 shows the energetically favourable region over the van der Waals surface of nifedipine with distinct hydrophobic fields lining the DHP and the 2'-nitrophenyl ring in position 4.

The same probe molecule (DRY) particularly identifies the Trp^{46} indole ring and *cis*-Pro^{47} of toxin FS_2 as being hydrophobic (Fig. 8). These directly connected amino acids are positioned in a well-defined type VIa *cis*-proline turn [27] stabilized by a hydrogen bond between the Met^{45} carbonyl oxygen and the Tyr^{48} amide hydrogen (Fig. 8).

The computation of the water accessibility of Trp^{46}-*cis*-Pro^{47} in each conformer results in surfaces from 190 to 220 $Å^2$, which means that, in relation to a minimized cyclic Trp-*cis*-Pro dipeptide, 68–80% of the surface is exposed on the outside of the toxin. To compare the hydrophobic regions, a manual superposition was performed using the grid fields as a template. Figure 9 shows the best fit of the fields and the common hydrophobic grid generated by GRAD [9]. In this superposition, the DHP ring is lying on top of the indole and the 2'-nitrophenyl alongside the *cis*-Pro pyrrolidine ring.

To detect further common properties of these molecules, the hydrogen donor and acceptor properties were calculated using different aliphatic hydroxyl probes: (i) without hydrogen donor; and (ii) without acceptor characteristics. Along this route, a clear differentiation between these features is possible, even if one or more common areas exist.

Nifedipine as a target molecule indicates strong hydrogen acceptor regions around the ester oxygens at C3 and C5 and the 2'-nitro group. A separate field is generated around the hydrogen in position 1 using the modified hydroxyl probe without hydrogen donor capacity (Fig. 10). Toxin FS_2 shows a pronounced hydrogen acceptor region in extension of the Trp^{46} carbonyl oxygen. A second region is observed around the carbonyl backbone oxygens of Ala^{44} and Tyr^{48}, which fits exactly the induced field of the sp carbonyl group of the superimposed nifedipine molecule (Fig. 11).

A closer examination reveals that this favourable interaction is possible in 13 conformations, although some of them present the carbonyl oxygen of Thr^{50} rather than those of Ala^{44} or Tyr^{48} as the acceptor group. A common hydrogen donor region is recognized in prolongation of the indole N-H (Fig. 11). In some conformers this feature is significantly increased by the positively charged Arg^{28} guanidinium side chain.

The fact that several DHPs without similarly strong hydrogen accepting groups in the 2'- or 3'-position are as potent as nifedipine (felodipine 2', 3'-Cl_2, amlodipine 2'-Cl or some 2'-CF_3 derivatives) indicates that this property of the 2'-nitro group is not essential. A second characteristic of this moiety is its strong negative potential, which is enforced by the ap oriented carbonyl oxygen of the C5 ester side chain.

The MEP of nifedipine shows large negative fields around the carboxyl oxygens and the 2'-nitro group, and a positive potential along the nitrogen in position 1 (Fig. 12). The MEP of toxin FS_2 contains two strong positive fields on top and at the turns of the loops, interrupted by a negatively charged belt in the middle of the molecule (Fig. 13). The pronounced positive potential in the lower part of the molecule is mainly generated by the positively charged Arg^{28} guanidinium side chain.

So as not to overestimate the potential due to this arginine side chain, whose flexibility was shown in the NMR study [12], a fragment of the toxin corresponding to Ala^{44}-Met^{45}-Trp^{46}-*cis*-Pro^{47}-Tyr^{48} was cut off and converted into the sequence *N*-Acetyl-Gly-Trp-*cis*-Pro-Ala-methylamide (Fig. 14). The atomic charges of this reduced fragment, containing all essential groups of the original sequence, were derived using an ab initio calculation [19]. To compare the electronic features of this amino acid stretch and nifedipine, the MEPs of the superimposed structures are shown in Fig. 14.

Two strong negative potentials (red clouds) are seen at each structure. The first one corresponds to the 2'-nitro and ap oriented ester oxygen of nifedipine and the Trp carbonyl oxygen of the toxin fragment (regions a). The second one is generated by the sp carbonyl oxygen of

nifedipine and the carbonyl oxygens of the *N*-acetyl group (corresponds to Ala[44]) and Ala (corresponds to Tyr[48]) of the fragment (regions b). A positive potential field (blue cloud) is observed in elongation of the DHP and the indole N-H bonds (regions c).

Discussion

AT-III toxins possess the same three-finger architecture as many other snake toxins. This motif represents a widespread topology of peptide toxins. However, in the venom of mambas also toxins are found resembling Dendrotoxin [28], which does not show the three-finger motif. On the other hand, this secondary structure is also observed in the saccharide-binding plant lectin wheat germ agglutinin [29] and the nontoxic xenoxins [30]. This clearly indicates that not the three-finger structure itself and its particular geometrical characteristics, but other structural properties are responsible for the effects.

The similarities of the pharmacological profiles [3–5] and the displacement studies of toxin FS_2 and different DHP derivatives [6] are indicators for a common binding site at L-type VGCC. The formation of the model is based on the fixed orientation of Trp[46]-*cis*-Pro[47] and the adjacent Met[45] and Tyr[48] by the type VIa *cis*-proline turn and by the similar hydrophobic, hydrogen bond forming, and electrostatic properties which are shared by this amino acid stretch of the AT-III toxins and nifedipine.

The formation of hydrogen bonds is observed in almost each cocrystallized enzyme–substrate complex, and seems to be one major component of the intermolecular stabilization at the binding site (for example, see dihydrofolate reductase–methotrexate [31]). For the rigid nifedipine molecule, the favourable hydrogen accepting regions are seen around the ester and the 2'-nitro groups. Even within the X-ray unit cell of nifedipine, these substituents serve as the accepting groups of the hydrogen in position 1 [20]. Considering the 20 conformers of the NMR experiment as 20 possible conformations of a dynamic equilibrium, it is understandable that in some conformations the maximal number of hydrogen bonds cannot be formed simultaneously. On the other hand, the probability of a hydrogen bond to be formed increases when acceptors and donors are fixed in optimum positions. Due to the possibility of temporary intramolecular hydrogen bond formation between the Trp[46] indole and the Thr[29] hydroxyl group, observed in three conformers, the orientation of the indole ring pointing backwards is favoured (Fig. 2). This side-chain orientation is observed in 18 conformations. Additional for the carbonyl oxygens of Ala[44] and Tyr[48], temporary intramolecular hydrogen bonds are possible which fix their positions. Even more restricted is the flexibility of the Trp[46] carbonyl oxygen. This atom is absolutely fixed in the turn, and points to the front. In the described situation where three regions of the toxin are fixed by (partially temporary) intramolecular forces, the same hydrogen bonding pattern as in nifedipine exists.

While intermolecular stabilization of ligands at their receptor sites by hydrogen bonds and especially by hydrophobic forces needs close contacts, complementary electrostatic potentials are essential for a long-range recognition according to the key and lock mode. An examination of the MEPs of toxin FS_2 and nifedipine indicates qualitatively similar electrostatic patterns, with the exception that the guanidinium moiety of the Arg[28] side chain induces a stronger positive field than the nifedipine DHP hydrogen in position 1 (see Figs. 12 and 13). At the same time, one of the negative potentials of toxin FS_2, induced by Ala[44] and Tyr[48] carbonyl oxygens, is more pronounced than the potential derived by the sp carbonyl oxygen of nifedipine (see Fig. 14, region b).

The results from Adachi et al. [32], indicating not a putative hydrogen bond on the C3 sp carbonyl oxygen but the antiperiplanar orientation of the C3 methyl ester side chain as being essential for the activity, could be a hint for the importance of the Met[45] side chain. Substitution of the nifedipine methyl against the most effective isopropyl ester [33] in this position would result in almost the same spatial orientation of this hydrophobic moiety as observed for the methionine side chain of the toxin (Fig. 2).

The exposed position at the tip of a stabilized loop (Fig. 15) allows the critical amino acids to reach their binding site, which seems to be located within the membrane and to be accessible to DHPs only from outside of the cell [34]. Even in the same genus, the three-finger-shaped cell adhesion protein dendroaspin [35] (isolated from the green mamba) has its essential recognition Arg-Gly-Asp (RGD) sequence (responsible for the glycoprotein IIB-IIIA (integrin $\alpha_{IIB}\beta_3$) antagonism [36]) at the tip of loop III as well. In addition, the same principle is observed at neuro- [37] and muscarinic toxins [38,39] showing their crucial residues at the tip of loop II.

Experimental results from Watanabe et al. [5], showing slightly different tissue selectivities for calciseptine and toxin FS_2, provide further evidence for the importance of the loop region. While calciseptine induces stronger relaxation on pre-contracted rat aortas, toxin FS_2 is more potent in the pulmonary artery. This small but significant difference must be caused by the substitution of only two amino acid residues (Fig. 5). In all three-finger toxins the function of sequence position 5 is the generation of an antiparallel β-sheet, whereas position 30 stabilizes the turn region in loop II. While serine (S) in toxin FS_2 and isoleucine (I) in calciseptine are mostly buried in the upper part of the nonessential loop I, the residue at position 30 is lying exposed, exactly aside the postulated crucial region at the tip of loop II. In addition, this residue is surrounded by the unique amino acids of AT-III

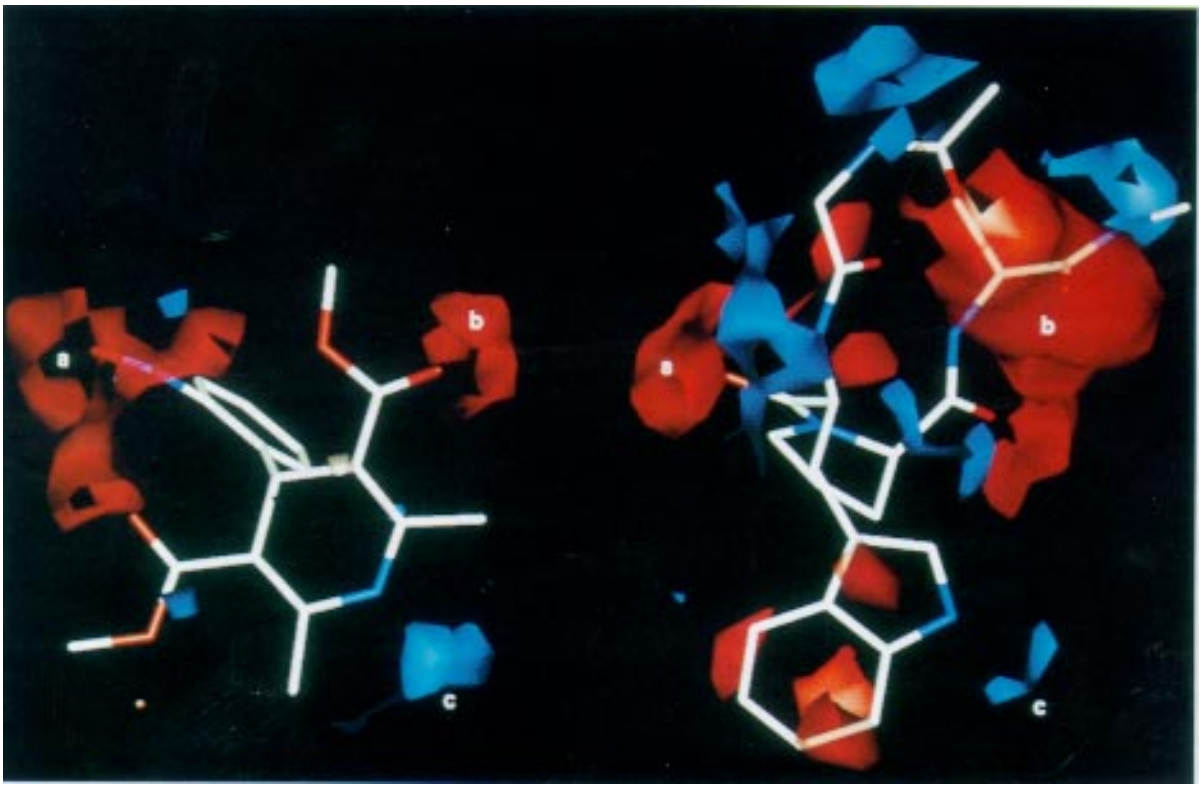

Fig. 14. MEPs of nifedipine (left) and the toxin fragment *N*-acetyl-Gly-Trp-*cis*-Pro-Ala-methylamide (right) in their parallel shifted superimposed positions. Red clouds indicate negative MEPs and blue clouds indicate positive MEPs contoured at ±1.5 kT/e. Common negative (regions a and b) and positive potentials (region c) are labelled (hydrogens are not shown).

Fig. 15. Superposition of nifedipine (yellow) and the Trp[46]-*cis*-Pro[47] residues of toxin FS_2 at the tip of loop III.

toxins (Fig. 2). The almost similar physicochemical properties of glutamine (Q) in calciseptine and histidine (H) in toxin FS_2 would not prevent the toxin's main effects, but could cause the different tissue selectivities.

Conclusions

In this theoretical study a comparison of the DHP derivative nifedipine and the black mamba toxin FS_2 was carried out to elucidate common molecular properties, which are essential for the binding at the VGCC. On the basis of the results, one can conclude the following:

(1) Both compounds reveal pronounced hydrophobic regions parallel to aromatic (nifedipine/FS_2: 2'-nitrophenyl/Trp[46] indole) and aliphatic ring systems (nifedipine/FS_2: DHP/*cis*-Pro[47] pyrrolidine ring), that are predestined for hydrophobic binding site interactions.

(2) Two hydrogen bond acceptor spaces (nifedipine/FS_2: (i) ap ester oxygen in conjunction with the 2'-nitro group/Trp[46] carbonyl oxygen; and (ii) sp ester oxygen/Ala[44] and Tyr[48] (Thr[50]) carbonyl oxygens) are observed in nifedipine and toxin FS_2.

(3) At the deepest place in regard to the superposition, both molecules possess a hydrogen donor group (nifedipine/FS_2: DHP/Trp[46] indole (Arg[28] guanidinium side chain) N-H).

(4) Qualitatively similar MEPs ensure the long-range recognition of nifedipine and the Met^{45}-Trp^{46}-*cis*-Pro^{47}-Tyr^{48} sequence of toxin FS_2 at the same receptor site.

(5) Additional hydrophobic interactions may be postulated for bulky substituents at the sp ester side chain of DHPs and the Met^{45} amino acid residue.

Although the 3D binding site of DHPs is still not known, site-directed mutagenesis experiments identify hydrophobic amino acid residues in the putative transmembrane segment IVS6 of VGCCs as the molecular determinants for high affinity DHP binding [40]. In accordance with this experimental finding, the above presented results strengthen the prediction of a lipophilic environment at the binding pocket, whereas the postulated electronic and hydrogen bond generating properties need to be substantiated by further investigations. For this purpose, one promising way to verify the binding hypothesis of toxin FS_2 would be the generation of site-directed toxin mutants. Following electrophysiological investigations would easily demonstrate the importance of each substituted essential amino acid in relation to its calcium channel blocking effect. Such an experimental confirmation could initiate the generation of smaller turn peptides showing the same properties as toxin FS_2, to serve as new leads for calcium channel modulating therapeutics.

Acknowledgements

I am grateful to Prof. Dr. H.-D. Höltje (Heinrich-Heine-Universität Düsseldorf, Germany) and Drs. H.R. Guy and S. Durell (National Institutes of Health, Bethesda, MD, U.S.A.) for helpful discussions, and thanks are due to the 'Ständige Kommission für Forschung und wissenschaftlichen Nachwuchs (FNK)' of the Freie Universität Berlin for financial support.

References

1 Strydom, D.J., Comp. Biochem. Physiol., 44B (1973) 269.
2 Karlsson, E., Mbugua, P.M. and Rodriguez-Ithurralde, D., Pharmacol. Ther., 30 (1985) 259.
3 De Weille, J.R., Schweitz, H., Maes, P., Tartar, A. and Lazdunski, M., Proc. Natl. Acad. Sci. USA, 88 (1991) 2437.
4 Teramoto, N., Ogata, R., Okabe, K., Kameyama, A., Kameyama, M., Watanabe, T.X., Kuriyama, H. and Kitamura, K., Pflüg. Arch. Eur. J. Physiol., 432 (1996) 462.
5 Watanabe, T.X., Itahara, Y., Kuroda, H., Chen, Y.-N., Kimura, T. and Sakakibara, S., Jpn. J. Pharmacol., 68 (1995) 305.
6 Yasuda, O., Morimoto, S., Chen, Y., Jiang, B., Kimura, T., Sakakibara, S., Koh, E., Fukuo, K., Kitano, S. and Ogihara, T., Biochem. Biophys. Res. Commun., 194 (1993) 587.
7 INSIGHT II/DISCOVER 2.9.7, Biosym/MSI, San Diego, CA, U.S.A.
8 GRID, v. 14, Molecular Discovery Ltd., Oxford, U.K.
9 Anzali, S., GRAD, Ph.D. Thesis, Freie Universität Berlin, Berlin, Germany, 1993.
10 DelPhi 2.50, Biosym/MSI, San Diego, CA, U.S.A.
11 Strydom, D.J., Eur. J. Biochem., 76 (1977) 99.
12 Albrand, J.-P., Blackledge, M.J., Pascaud, F., Hollecker, M. and Marion, D., Biochemistry, 34 (1995) 5923.
13 Sander, C. and Schneider, R., Proteins, 9 (1991) 56.
14 Rost, B., Methods Enzymol., 266 (1996) 525.
15 Bairoch, A. and Boeckmann, B., Nucleic Acids Res., 22 (1994) 3578.
16 Bernstein, F.C., Koetzle, T.F., Williams, G.J.B., Meyer, E.F., Brice, M.D., Rodgers, J.R., Kennard, O., Shimanouchi, T. and Tasumi, M., J. Mol. Biol., 112 (1977) 535.
17 Laskowski, R.A., MacArthur, M.W., Moss, D.S. and Thornton, J.M., J. Appl. Crystallogr., 26 (1993) 283.
18 Connolly, M.L., J. Appl. Crystallogr., 16 (1983) 548.
19 SPARTAN 3.0, Wavefunction, Irvine, CA, U.S.A.
20 Triggle, A.M., Shefter, E. and Triggle, D.J., J. Med. Chem., 23 (1980) 1442.
21 Cambridge Structural Database, Cambridge Crystallographic Data Center, Cambridge, U.K.
22 Rovnyak, G.C., Kimball, S.D., Beyer, B., Cucinotta, G., DiMarco, J.D., Gougoutas, J., Hedberg, A., Malley, M., McCarthy, J.P., Zhang, R. and Moreland, S., J. Med. Chem., 38 (1995) 119.
23 Höltje, H.-D. and Marrer, S., J. Comput.-Aided Mol. Design, 7 (1988) 174.
24 Schleifer, K.-J., Pharm. Pharmacol. Lett., 5 (1995) 162.
25 Ramachandran, G.N. and Sasisekharan, V., Adv. Protein Chem., 23 (1968) 283.
26 Ali, S.L., In Florey, K. (Ed.) Analytical Profiles of Drug Substances, Vol. 18, Academic Press, San Diego, CA, U.S.A., 1989, pp. 221–288.
27 Richardson, J., Adv. Protein Chem., 34 (1981) 167.
28 Swaminathan, P., Hariharan, M., Murali, R. and Singh, C.U., J. Med. Chem., 39 (1996) 2141.
29 Drenth, J., Low, B.W., Richardson, J.S. and Wright, C.S., J. Biol. Chem., 255 (1980) 2652.
30 Kolbe, H.V.J., Huber, A., Cordier, P., Rasmussen, U.B., Bouchon, B., Jaquinod, M., Vlasak, R., Délot, E.C. and Kreil, G., J. Biol. Chem., 268 (1993) 16458.
31 Matthews, D.A., Alden, R.A., Bolin, J.T., Freer, S.T., Xuong, N., Kraut, J., Poe, M., Williams, M. and Hoogsteen, K., Science, 197 (1977) 452.
32 Adachi, I., Yamamori, T., Hiramatsu, Y., Sakai, K., Mihara, S., Kawakami, M., Masui, M., Uno, O. and Ueda, M., Chem. Pharm. Bull., 36 (1988) 4389.
33 Goldmann, S. and Stoltefuss, J., Angew. Chem., 103 (1991) 1587.
34 Kass, R.S., Arena, J.P. and Chin, S., J. Gen. Physiol., 98 (1991) 63.
35 Sutcliffe, M.J., Jaseja, M., Hyde, E.I., Lu, X. and Williams, J.A., Nat. Struct. Biol., 1 (1994) 802.
36 Ruoslahti, E. and Pierschbacher, M.D., Cell, 44 (1986) 517.
37 Pillet, L., Trémeau, O., Ducancel, F., Drevet, P., Zinn-Justin, S., Pinkasfeld, S., Boulain, J.-C. and Ménez, A., J. Biol. Chem., 268 (1993) 909.
38 Jolkonnen, M., Adem, A., Hellmann, U., Wernstedt, C. and Karlsson, E., Toxicon, 33 (1995) 399.
39 Jolkonnen, M., Van Giersbergen, P.L.M., Hellmann, U., Wernstedt, C., Oras, A., Satyapan, N., Adem, A. and Karlsson, E., Eur. J. Biochem., 234 (1995) 579.
40 Peterson, B.Z., Tanada, T.N. and Catterall, W.A., J. Biol. Chem., 271 (1996) 5293.